

Radiative $b \rightarrow d$ Penguins

P. Bechtle^a

Stanford Linear Accelerator Center, 2575 Sand Hill Road, Menlo Park, CA 94025, USA^b

Abstract

This article gives an overview of the recent searches and measurements of $b \rightarrow d$ penguin transitions with the BaBar experiment. The branching fraction of these decays in the Standard Model (SM) is expected to be a factor of 10 or more lower than the corresponding $b \rightarrow s$ penguin transitions, but a deviation from the SM prediction would be an equally striking sign of new physics. The exclusive decay $B \rightarrow \pi \ell \ell$ is searched by BaBar with no excess over the background found. The BaBar measurement of $B \rightarrow (\rho, \omega) \gamma$ provides the first evidence of $B^+ \rightarrow \rho^+ \gamma$,^c is in good agreement with the previous Belle results and provides a measurement of $|V_{td}/V_{ts}|$ independent of the one from B_s mixing. No deviation from the SM is found.

1 Introduction

Since the first ≈ 10 radiative penguin decays of B mesons have been reported by CLEO in 1993¹, the measurements of radiative penguins at the B factory experiments BaBar and Belle have expanded into a rich field of physics. As many as 15 individual exclusive $b \rightarrow s$ modes have been observed and some of the corresponding branching fractions have been measured with a precision of about 10 %. This makes it possible to test SM predictions of these rare decays, e.g. QCD calculations of form factors. Additionally, the inclusive measurement of $b \rightarrow s \gamma$ allows strong constraints on new physics models² and precision measurements of heavy quark effective theory predictions.

With the success of the $b \rightarrow s$ penguin measurements in hand, the next step is to explore $b \rightarrow d$ penguins, which due to Cabbibo suppression are not only about one order of magnitude more rare, but also face a much more severe background due to the abundance of pions in the background. This paper gives an overview of the recent results from BaBar for the exclusive modes $B \rightarrow \pi \ell \ell$ and $B \rightarrow (\rho, \omega) \gamma$. Section 2 will briefly discuss the interest in these measurements from the point of view of the search for new physics, Sections 3 and 4 will summarize the measurements, and discuss the measurement of $|V_{td}/V_{ts}|$ from $\mathcal{B}(B \rightarrow (\rho, \omega) \gamma)$.

2 New Physics in Radiative Penguins

The beauty of the search for new physics in penguin decays lies in the fact that the dominating diagram in the SM is a loop or box diagram with heavy particles in the loop. This is exem-

^afor the BaBar collaboration

^bnow: DESY, Notkestraße 85, 22607 Hamburg, Germany, philip.bechtle@desy.de

^ccharge conjugation is implied everywhere in this paper, if not stated otherwise

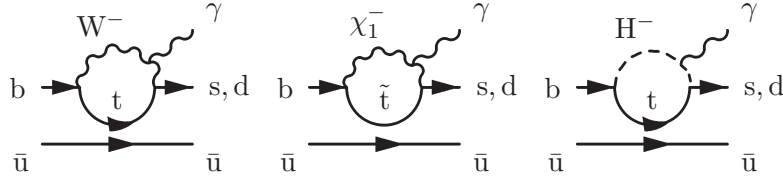


Figure 1: *New Physics in Radiative Penguins.* The left graph shows the SM contribution, the middle graph a possible SUSY contribution at the same loop level and with similar order of magnitudes of the couplings and masses. The right graph shows a SUSY or 2HDM contribution.

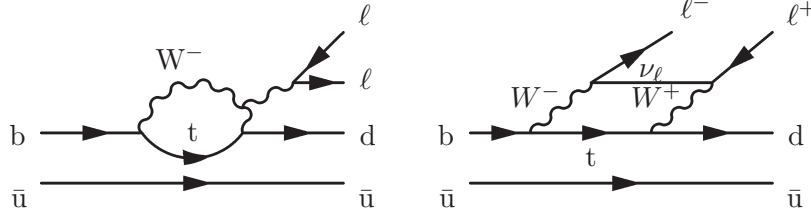


Figure 2: *The dominating $b \rightarrow d\ell\ell$ penguin graphs in the SM.* Similar new physics contributions as in Fig. 1 apply.

plified in Figure 1. Possible new physics, Supersymmetry (SUSY) or the two-Higgs Doublet Model (2HDM) in this case, contribute with particles in the same mass range of 100 to several hundred GeV and often also with similar couplings. This allows strong constraints on new physics models. However, while the measurement of exclusive decays is often experimentally clean, the interpretation of the experimental results for very rare exclusive decays often suffers from theoretical uncertainties in the prediction of form factors, radiative corrections, and other suppressed graphs. Still, strong constraints and precise SM measurements can be gained from ratios of branching fractions.

3 $b \rightarrow d\ell^+\ell^-$ Transitions

The smallest B branching fractions measured up to now are the $b \rightarrow s$ modes $\mathcal{B}(B \rightarrow K\ell\ell) = (3.4 \pm 0.7 \pm 0.2) \times 10^{-7}$ and $\mathcal{B}(B \rightarrow K^*\ell\ell) = (7.8 \pm 1.9 \pm 1.1) \times 10^{-7}$.³ In comparison to that, $\mathcal{B}(B \rightarrow \pi\ell\ell)$ is expected to be suppressed by $|V_{td}/V_{ts}|^2$, with the most recent prediction of $\mathcal{B}(B \rightarrow \pi\ell\ell) = 3.3 \times 10^{-8}$.⁴ Any deviation from this order of magnitude would be a striking sign of new physics. The two dominating diagrams for this transition are shown in Figure 2, showing one penguin and one W box diagram.

The BaBar analysis⁵ on a dataset of 209 fb^{-1} faces another experimental challenge with respect to $B \rightarrow K\ell\ell$ in addition to the reduced branching fraction, namely the much higher rate of π in the background than K . The analysis strategy is to first select clean π , e and μ candidates and then veto resonances decaying into $\ell\ell$. The $u\bar{u}$, $d\bar{d}$, $s\bar{s}$ events are strongly reduced by requiring two $p > 1 \text{ GeV}$ leptons in the Event. The charmonium veto against $B \rightarrow J/\psi(\psi')\pi(K^*)$ events is shown in Figure 3 (a). The tilt in the mass veto stems from the fact that events with bremsstrahlung of one of the leptons are off both in mass and in reconstructed energy, visible in $\Delta E = E_B - 1/2 E_{Beam}$. Event shape variables against continuum events are grouped in a Fisher discriminant, and event shape variables against $B\bar{B}$ background events are grouped into a likelihood. After these cuts, only combinatoric background from $c\bar{c}$ and $B\bar{B}$ events are left.

Backgrounds are controlled with various control samples ($e\mu$, $B \rightarrow J/\psi(\psi')\pi(K^*)$). Hadronic mistags are measured in a separate study by inverting the hadron vetos and then imposing the measured mistag rates as event weights. The resulting small peaking background fraction is shown in Figure 3 (b) with $\pi^+h^+h^-$ on the left and $\pi^0h^+h^-$ on the right side. Finally, the background in the m_{ES} and ΔE sidebands is extrapolated into the signal region (see Figure 4) to assess the background level independent of the MC simulation.

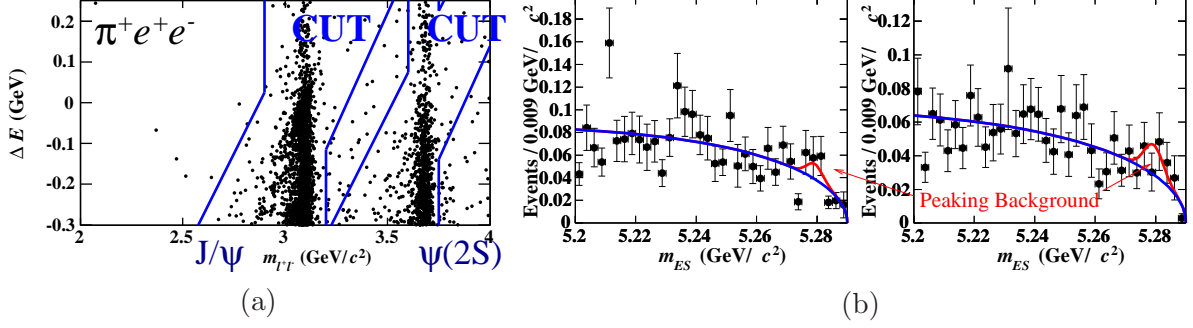


Figure 3: In (a), the $m_{\ell\ell}, \Delta E$ distribution with the charmonium vetos in the $B \rightarrow \pi\ell\ell$ analysis is shown. (b) shows the peaking background determination in $B^0 \rightarrow \pi^0\ell\ell$ (left) and $B^+ \rightarrow \pi^+\ell\ell$ (right)

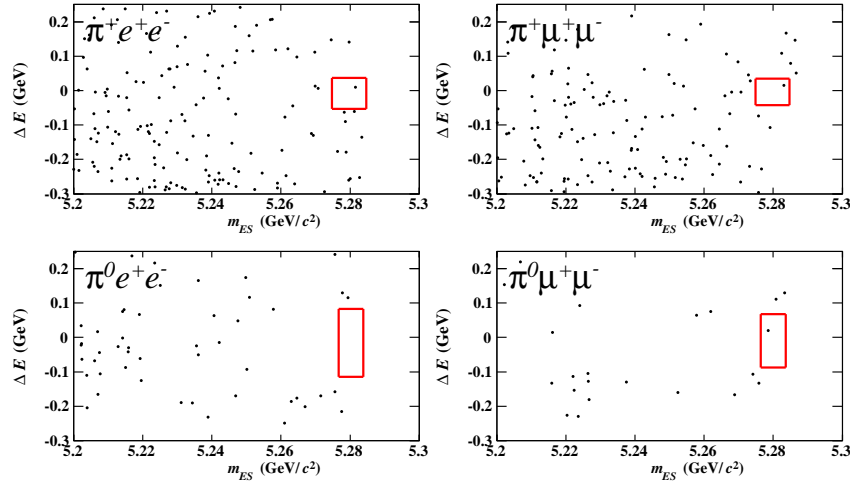


Figure 4: Results of the $B \rightarrow \pi\ell\ell$ analysis in the different modes in the $m_{ES}, \Delta E$ plane. The signal boxes are shown in red.

No excess over the background is observed, hence limits are set using a frequentist cut-and-count method in the signal boxes. The resulting limit of $\mathcal{B}(B \rightarrow \pi\ell\ell) = 3.3 \times 10^{-8}$ assuming isospin symmetry is within a factor of 3 of the SM prediction. A detailed summary of the results can be found in Table 1.

4 $b \rightarrow d\gamma$ Transitions

$b \rightarrow d\gamma$ penguins have been first observed by Belle with 350 fb^{-1} with evidence for the $B^0 \rightarrow \rho^0\gamma$ mode⁶. In addition to the possibility of finding new physics if the measured branching fractions exceed $\approx 0.5 \times 10^{-6}$ for the neutral mode or $\approx 1 \times 10^{-6}$ for the charged mode significantly, it offers the important possibility to measure $|V_{td}/V_{ts}|$ via

$$\frac{\Gamma(B \rightarrow \rho\gamma)}{\Gamma(B \rightarrow K^*\gamma)} = \left| \frac{V_{td}}{V_{ts}} \right|^2 \frac{(m_B - m_\rho)^3}{(m_B - m_{K^*})^3} \left(\frac{T^\rho(0)}{T^{K^*}(0)} \right)^2 (1 + \Delta R), \quad (1)$$

with $\Delta R = 0.1 \pm 0.1$ ⁷ containing radiative corrections and sub-dominant helicity suppressed W -fusion diagrams (hence depending on V_{ub} and the CKM fit itself and thus not uncorrelated from $|V_{td}/V_{ts}|$), and a form-factor ratio of $T^{K^*}(0)/T^\rho(0) = 1.17 \pm 0.09$ ⁸. The graphs involved here are expected to have completely independent possible new physics contributions than $\Delta m_d/\Delta m_s$, hence the comparison of the two results is very important.

Table 1: Results of the $B \rightarrow \pi \ell \ell$ selection and limits on the branching fraction inferred from the absence of an excess over the SM background.

PRELIMINARY		exp.	BF UL
Mode	obs.	backg.	90 % CL (10^{-7})
$B^\pm \rightarrow \pi^\pm \ell \ell$	2	1.86 ± 0.38	1.17
$B^0 \rightarrow \pi^0 \ell \ell$	1	0.71 ± 0.30	1.15
isospin combination			0.91
$B \rightarrow \pi e \mu$	1	2.77 ± 0.70	0.92

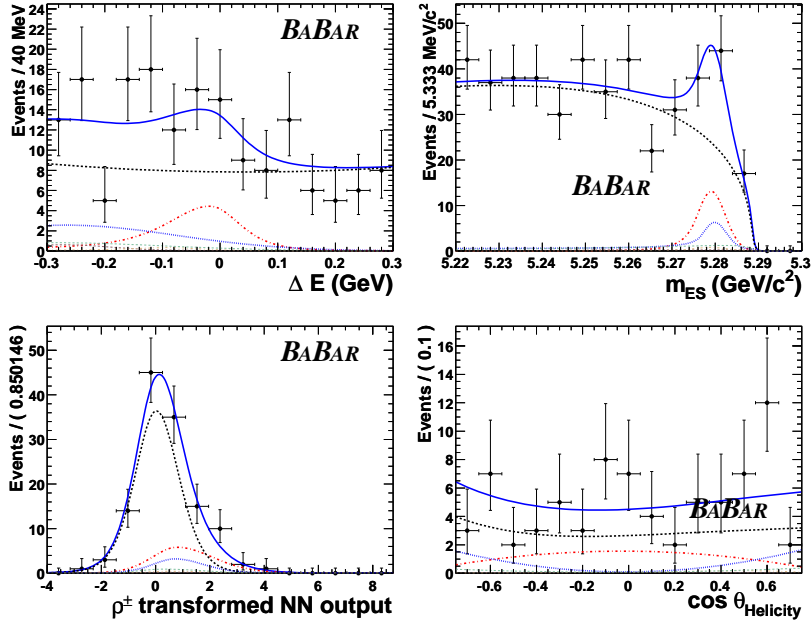


Figure 5: Extraction of the signal in the $B \rightarrow \rho/\omega \gamma$ analysis in the $B^+ \rightarrow \rho^+ \gamma$ channel in a four-dimensional simultaneous extended maximum likelihood fit. The signal is shown dash-dotted (red), the continuum is dashed (black), the total B background is shown dotted (blue).

Here, the experimental challenge lies not only in the particle ID requirements to suppress K background, but also in the π combinatorics coming from the wide resonance states ($\Gamma(\rho) = 150 \text{ MeV}$) and the high photon background from continuum events with $\pi^0/\eta \rightarrow \gamma\gamma$. The BaBar analysis⁹ on 316 fb^{-1} of data tackles this challenge by a likelihood veto against π^0/η based on the invariant mass of the photon pair and the energy of the lower energetic photon, improving the veto significantly over a simple cut on $m_{\gamma\gamma}$. Additionally, a Neural Net (NN) based continuum suppression is applied.

To extract the result, a simultaneous maximum-likelihood fit is performed to m_{ES} , ΔE , the NN output and $\cos \theta_{\text{hel}}$, where θ_{hel} is the helicity angle of the vector meson ρ or ω , which are transversely polarized in signal events. For ω , the Dalitz angle of the ω decay is used additionally. An example fit is shown for the $B^+ \rightarrow \rho^+ \gamma$ mode in Figure 5. Many control sample checks are performed. With off-peak data used to control the continuum simulation, and $B \rightarrow K^* \gamma$ and $B \rightarrow D\pi$ used to control resolutions and efficiencies.

The result for the individual modes and different combinations is shown in Table 2. While the $B^0 \rightarrow \omega \gamma$ signal is not yet significant on its own, this result represents the first evidence for $B^+ \rightarrow \rho^+ \gamma$. Figure 6 shows the good agreement of the results with the SM predictions and the agreement with the earlier Belle results. The result for the isospin combination $B \rightarrow \rho/\omega \gamma$ is to be taken with care, however, since the ω does not belong to the isospin triplet.

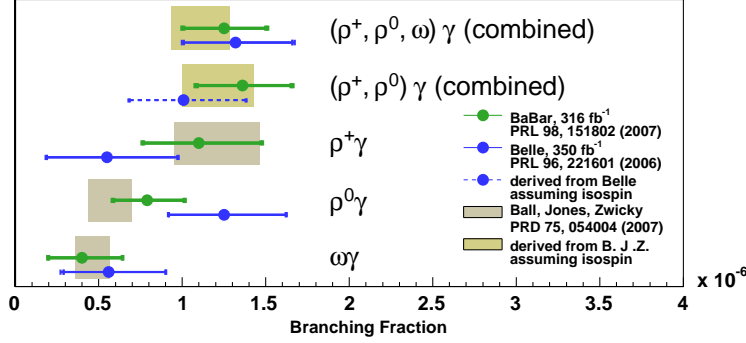


Figure 6: Graphical representation of the results of the Belle and Babar measurements of $b \rightarrow d\gamma$ penguins and the comparison with the SM prediction.

Table 2: Results of the BaBar $B \rightarrow (\rho/\omega)\gamma$ analysis in terms of extracted branching fraction and significance. The isospin combination is shown in the last line.

Mode	Result	Significance
$\mathcal{B}(B^\pm \rightarrow \rho^\pm \gamma)$	$(1.1^{+0.37}_{-0.33} \pm 0.09) \times 10^{-6}$	3.8σ
$\mathcal{B}(B^0 \rightarrow \rho^0 \gamma)$	$(0.79^{+0.22}_{-0.20} \pm 0.06) \times 10^{-6}$	4.9σ
$\mathcal{B}(B^0 \rightarrow \omega \gamma)$	$(0.40^{+0.24}_{-0.20} \pm 0.05) \times 10^{-6}$	2.2σ
combination of all modes		
$\mathcal{B}(B \rightarrow \rho/\omega \gamma)$	$(1.25^{+0.25}_{-0.24} \pm 0.09) \times 10^{-6}$	6.4σ

The results of $\mathcal{B}(B \rightarrow \rho/\omega \gamma)$ can be used to extract $|V_{td}/V_{ts}|$ using Eq. 1. Using the world average of $\mathcal{B}(B \rightarrow \rho/\omega \gamma) = (1.25^{+0.25}_{-0.24} \pm 0.09) \times 10^{-6}$, a value of $|V_{td}/V_{ts}|_{\rho/\omega \gamma} = 0.202^{+0.017}_{-0.016} \pm 0.015$ ¹⁰ can be extracted, in very good agreement with the result obtained from $\Delta m_d/\Delta m_s$ of $|V_{td}/V_{ts}|_{\Delta m_d/\Delta m_s} = 0.2060 \pm 0.0007^{+0.0081}_{-0.0060}$ from the Tevatron¹¹. While the precision from $B \rightarrow \rho/\omega \gamma$ is not sufficient to compete with $\Delta m_d/\Delta m_s$, it provides an important independent check of possible new physics, due to the different nature of the possible new physics contributions in the two processes. A comparison of the two results with the CKM fit and the imposed constrained in the $\bar{\rho}, \bar{\eta}$ plane of the CKM parameterization can be found in Fig. 7.

5 Summary and Outlook

With the extraordinary luminosities of the B-factories Belle and BaBar, the field of strange radiative penguin decays of the B meson has evolved into one of the most important areas of precision measurements in the search of new physics. While it is still unclear whether $B \rightarrow \pi \ell \ell$ transitions will be seen in the lifetime of the present B-factories, the rare decay $b \rightarrow d\gamma$ has now been seen by Belle and BaBar, and these measurements will possibly evolve towards precision measurements in the same way as the $b \rightarrow s\gamma$ decays before. With the anticipated $\mathcal{L}_{\text{int}} \approx 1 \text{ ab}^{-1}$ of luminosity per B-factory at the end of 2008, a $\approx 10\%$ measurement of the CP asymmetry in $B \rightarrow \rho/\omega \gamma$ should be feasible. Another interesting measurement would be the isospin asymmetry $A_I = 2\Gamma(B^0 \rightarrow \rho^0 \gamma)/\Gamma(B^\pm \rightarrow \rho^\pm \gamma) - 1$, which presents a completely new way of obtaining a measurement of the CKM-angle γ , as outlined in¹⁰ and shown in Fig. 8.

Acknowledgments

The author would like to thank the PEP-II accelerator and its crew for the excellent luminosity delivered to BaBar, and the radiative penguin analysis group in BaBar for lots of support and

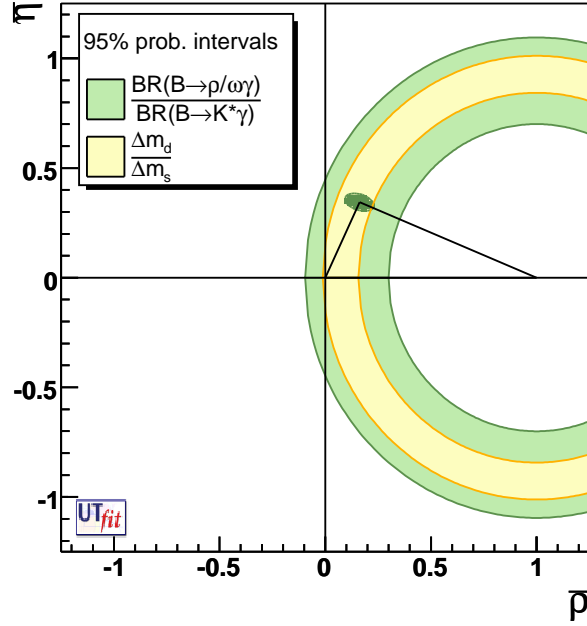


Figure 7: The constraint on $|V_{td}/V_{ts}|$ from $B \rightarrow \rho/\omega\gamma$ and $\Delta m_d/\Delta m_s$ in the $\bar{\rho}$, $\bar{\eta}$ plane and the comparison with the SM CKM fit.

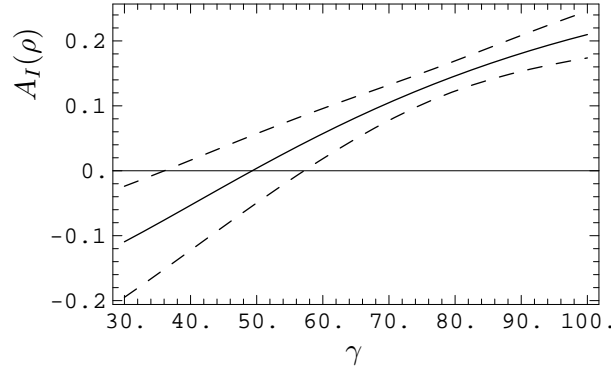


Figure 8: A possible new constraint on the CKM-angle γ from the isospin asymmetry measurement in $B \rightarrow \rho\gamma$.

very lively discussions.

References

1. R. Ammar *et al.* [CLEO Collaboration], Phys. Rev. Lett. **71** (1993) 674.
2. see e.g. M. Misiak *et al.*, Phys. Rev. Lett. **98** (2007) 022002 and references therein.
3. B. Aubert *et al.* [BABAR Collaboration], Phys. Rev. D **73** (2006) 092001.
4. T. M. Aliev and M. Savci, Phys. Rev. D **60**, 014005 (1999).
5. B. Aubert *et al.* [BABAR Collaboration], arXiv:hep-ex/0703018, submitted to PRL.
6. K. Abe *et al.* [BELLE Collaboration], Phys. Rev. Lett. **96** (2006) 221601.
7. A. Ali, E. Lunghi and A. Y. Parkhomenko, Phys. Lett. B **595**, 323 (2004).
8. P. Ball and R. Zwicky, JHEP **0604**, 046 (2006).
9. B. Aubert *et al.* [BABAR Collaboration], Phys. Rev. Lett. **98** (2007) 151802.
10. P. Ball, G. W. Jones and R. Zwicky, Phys. Rev. D **75** (2007) 054004.
11. A. Abulencia *et al.* [CDF Collaboration], Phys. Rev. Lett. **97**, 242003 (2006).